Prion 8:4, 314–318; July/August 2014; © 2014 Taylor & Francis Group, LLC

Pressure-assisted dissociation and degradation of "proteinase K-resistant" fibrils prepared by seeding with scrapie-infected hamster prion protein

Kazuyuki Akasaka[1,2,*], Akihiro Maeno[2], Taichi Murayama[1], Hideki Tachibana[1,2], Yuzo Fujita[2], Hitoki Yamanaka[3], Noriyuki Nishida[3], and Ryuichiro Atarashi[3]

[1]Graduate School of Biology-Oriented Science and Technology; Kinki University; Kinokawa, Japan; [2]High Pressure Protein Research Center; Institute of Advanced Technology; Kinki University; Kinokawa, Japan; [3]Department of Molecular Microbiology and Immunology; Graduate School of Biomedical Sciences; Nagasaki University; Nagasaki, Japan

Keywords: Recombinant Hamster prion protein, proteinase K-resistant prion fibrils, pressure-assisted dissociation, dissociation of prion fibrils, enzymatic degradation of prion fibrils, Western blotting

Abbreviations: PK, proteinase K; PrP^C, cellular form of prion protein; PrP^{Sc}, scrapie form of prion protein; rHaPrP, recombinant Hamster prion protein; $rHaPrP^{res}$, PK-resistant recombinant Hamster prion protein; AFM, atomic force microscopy; QUIC, quaking-induced conversion.

The crucial step for the fatal neurodegenerative prion diseases involves the conversion of a normal cellular protein, PrP^C, into a fibrous pathogenic form, PrP^{Sc}, which has an unusual stability against heat and resistance against proteinase K digestion. A successful challenge to reverse the reaction from PrP^{Sc} into PrP^C is considered valuable, as it would give a key to dissolving the complex molecular events into thermodynamic and kinetic analyses and may also provide a means to prevent the formation of PrP^{Sc} from PrP^C eventually in vivo. Here we show that, by applying pressures at kbar range, the "proteinase K-resistant" fibrils ($rHaPrP^{res}$) prepared from hamster prion protein (rHaPrP [23–231]) by seeding with brain homogenate of scrapie-infected hamster, becomes easily digestible. The result is consistent with the notion that $rHaPrP^{res}$ fibrils are dissociated into rHaPrP monomers under pressure and that the formation of PrP^{Sc} from PrP^C is thermodynamically controlled. Moreover, the efficient degradation of prion fibrils under pressure provides a novel means of eliminating infectious PrP^{Sc} from various systems of pathogenic concern.

Introduction

The crucial step for the fatal neurodegenerative prion diseases involves the transformation of a normal cellular protein, PrP^C, into a fibrous pathogenic form of the protein, PrP^{Sc}, either sporadically or by infection.[1] The transformation of PrP^C into PrP^{Sc} is a slow process in vivo and, once formed, the fibril shows an exceptionally high stability against heat treatment[2] and high resistivity against enzymatic proteolysis.[3] Thus the transformation is considered practically irreversible, prohibiting the study how PrP^{Sc} is thermodynamically and kinetically related to its normal precursor PrP^C, one of the fundamental questions in pursuing the cause of prion disease, and use the relationship for efficient removal of PrP^{Sc}.

Pressure has proven to be a generally useful perturbation for investigating protein conformational equilibrium, particularly as it covers a wide dynamic range of conformation, namely from folded to unfolded of a globular protein[4] as well as from monomers to oligomers in protein assembly.[5] In general, if a protein exists in solution in an equilibrium mixture of conformational states mutually differing in partial molar volume ΔV,[4] pressure shifts their equilibrium in favor of the lower volume states and increasing the relative population of the latter often dramatically by a factor $\sim\exp(-P\Delta V/RT)$.[5,6] Although no information is available on the volumetric property of Hamster rPrP in its monomeric and fibrous states, the study on Murine PrP showed that aggregated β-sheet-rich MrPrP [23–231] undergoes unfolding with $\Delta V = -43.6$ ml mol^{-1}.[7] Furthermore, in view of the fact that rPrP oligomers of human prion protein is dissociable under pressure,[8] meaning $\Delta V = V_{monomer} - V_{oligo} < 0$ and that hen lysozyme and its mutant are distinctly more voluminous in the amyloid protofibril state than in its naturally denatured monomeric state, $\Delta V = V_{monomer} - V_{fibril} < 0$,[9-13] we expect that under closely physiological conditions the volume is lower for the rPrP monomer, namely, $\Delta V = V_{monomer} - V_{fibril} < 0$. Furthermore, we found that the shrinking of the protofibril undergoes

*Correspondence to: Kazuyuki Akasaka; Email: akasaka@waka.kindai.ac.jp
Submitted: 05/02/2014; Revised: 07/02/2014; Accepted: 07/19/2014
http://dx.doi.org/10.4161/pri.32081

by the dissociation of a monomeric species at the growing end of the fibril,[12] i.e., by obeying the linear polymerization mechanism in which the fibril and the monomer are in dynamic equilibrium.[13] Thus we have ample reasons to expect that the application of pressure to a solution containing PrP fibrils would shift the equilibrium toward dissociation, increasing the equilibrium concentration of PrP monomers, PrP^C, which, in the presence of proteinase K (PK), would be readily degraded into smaller fragments. The pressure-enhanced degradation of fibrils may be evaluated at 0.1 MPa after certain period of the reaction, by monitoring the diminishing number of fibrils with an atomic force microscopy (AFM) and their degradation into peptide fragments by western blotting.

Results and Discussion

Figure 1 illustrates the actual experimental procedure employed in the present work. Instead of directly working on PrP^{Sc} in vivo, we choose, at this stage, to work with proteinase K-resistant fibrils ($rHaPrP^{res}$), which is prepared from recombinant hamster PrP (rHaPrP [23–231]) in vitro by seeding with brain homogenate of scrapie-infected hamster under quaking, or by QUIC (quaking-induced conversion),[14] the process mimicking the conversion of cellular PrP^C into PrP^{Sc}. The automated shaking was performed on the solution containing rHaPrP for 24 h at 37 °C in 0.5 M Gdn-HCl, 150 mM NaCl, 150 mM HEPES buffer, pH7.0, in the presence of diluted brain homogenate of the hamster that had been infected with PrP^{Sc} from sheep. Because of the high effective molecular weight of the fibrils and the small quantity of the protein available for analysis (<1μg) at one time, we employed AFM and western blotting, both of which are capable of detecting a small quantity of proteins (<1μg) without using high pressure NMR spectroscopy.[8,15] The former gives a direct image, though qualitative, on what happens to $rHaPrP^{res}$ fibrils, while the latter should give the degradation process more quantitatively.

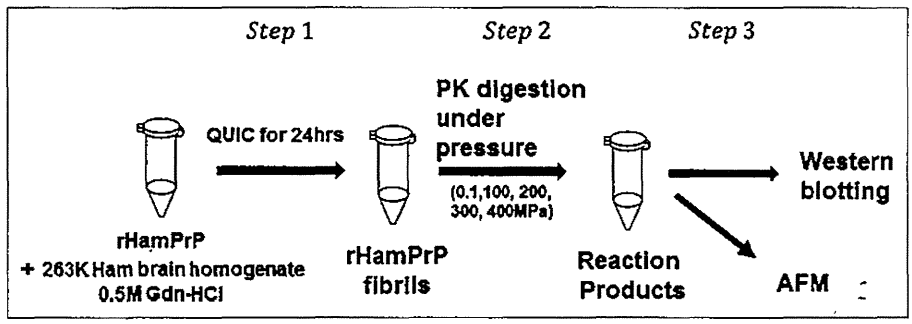

Figure 1. Illustration of the experimental procedure in the present work. Step1: rHamPrP was treated with brain homogenate of scrapie-infected hamster 263K brain homogenate to produce rHamPrP fibrils (the method of QUIC[14]). Step 2: rHamPrP fibrils were treated with proteinase K under different pressures at 25 °C. Step 3. The reaction products were subjected to analysis with western blotting and AFM. See Materials and Methods for more details.

Figure 2, far left, shows a representative AFM image of the $rHaPrP^{res}$ fibrils as prepared. The fibrils exhibit a heterogeneously aggregated morphological feature, similar to those reported for other prion fibrils.[16] The rest of the figures show representative AFM images of $rHaPrP^{res}$ fibrils treated with a high dose of PK for 1 h at pH 7.0 at 25 °C under different pressure conditions (0.1~400 MPa). By treatment at 0.1 MPa for 1 h, fibrils remain, but effects were found on their shapes (Fig. 2, second from the left). By treatment with PK at increasing pressures, the fibrils diminish dramatically and disappear completely at 400 MPa (Fig. 2, far right).

Figure 3 shows the western blotting patterns of the solution of monomeric rHaPrP' (PrP^C) (A) and those of the solution of $rHaPrP^{res}$ fibrils (B), treated similarly with a high dose of PK for 1 h at pH 7.0 at 25 °C under different pressure conditions (0.1~400 MPa). For rHaPrP (PrP^C) (Fig. 3A), we note that the digestion by PK proceeds almost fully even at 0.1 MPa, but becomes complete above 100MPa. The accelerated digestion of monomeric proteins with a proteinase under pressure follows the general mechanism proposed for pressure-accelerated degradation of proteins.[17] For $rHaPrP^{res}$ fibrils (Fig. 2B), we note that, at 0.1 MPa, the original 25 kDa band is replaced with the strong ~12 kDa bands, indicating that residues 23 to 140 including the N-terminal flexible segment of $rHaPrP^{res}$ are selectively cleaved off, leaving fibrils consisting of "truncated" $rHaPrP^{res}$ monomers with only the C-terminal core part (residues ~140–231).[3,14] This process of limited proteolysis of $rHaPrP^{res}$ is schematically illustrated in Figure 4A, in which the PK-resistant core parts of $rHaPrP^{res}$ are shown by gray column.

What is dramatic is the degradation of the ~12 kDa bands, corresponding to the core part of rHaPrP, which start diminishing by treatment with PK at elevated pressures at 300–400 MPa (Fig. 3B, right). The result clearly indicates that $rHaPrP^{res}$ fibrils are fully degraded into smaller peptide fragments by PK at elevated pressures. This result is consistent with the notion that $rHaPrP^{res}$ is dissociated into monomeric species under the elevated pressures, while PK remains active. The activity of PK at pressures (100–400 MPa) is verified by Figure 3A, in which an efficient degradation of rHaPrP (PrP^C) with PK at 100–400 MPa is shown. The dramatic process of PK-degradation of $rHaPrP^{res}$ fibrils (PrP^{Sc}) is schematically illustrated in Figure 4B, in which the fibrillar PrP^{Sc} is dissociated into monomeric PrP^C under elevated pressures, followed immediately by the efficient degradation of PrP^C by proteinase K.

The entire process described above may be more adequately described thermodynamically in the following manner: The PrP fibrils (PrP^{Sc}) and PrP monomers, namely PrP^C, are basically in dynamic equilibrium ($PrP^{Sc} \rightleftharpoons PrP^C$). At 0.1 MPa, the equilibrium is strongly shifted toward the

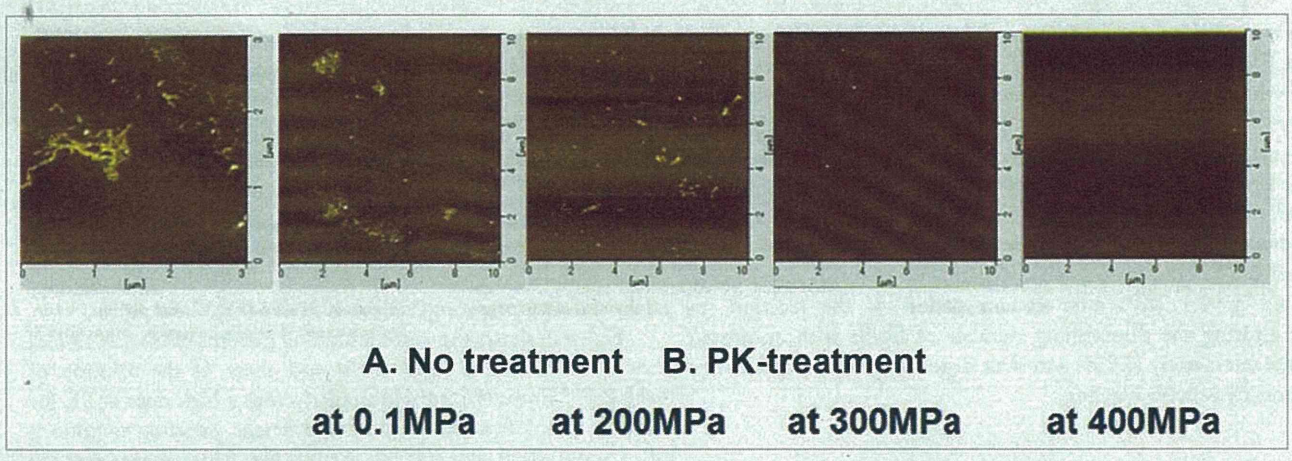

Figure 2. Atomic force microscopy images of rHaPrP^{res} fibrils PK-treated under different conditions. (**A**) A representative image of rHaPrP^{res} fibrils as prepared by the method of QUIC[14]. (**B**) Representative images of rHaPrP^{res} fibrils after PK-treatment for 1 h at respective pressures. See Materials and Methods for more details.

former (PrP^{Sc}). Under applied pressure, the equilibrium will be shifted more in favor of the latter (PrP^{C}) by a factor anticipated by $\sim\exp(-P\Delta V/RT)$ with a negative value of $\Delta V = V_{monomer} - V_{fibril} < 0$.[5,6] The lower volume of the latter state (PrP^{C}) would further be substantiated under pressure by pressure unfolding of PrP^{C} (PrP^{C}[folded] $\rightleftharpoons$ PrP^{C}[unfolded]).[17] The increased equilibrium population of PrP monomers, PrP^{C}, under pressure would render the PrP fibrils degraded continually until they disappear totally, thanks to the dynamic equilibrium $PrP^{Sc} \rightleftharpoons PrP^{C}$(folded) $\rightleftharpoons$ PrP^{C}(unfolded).

Implication of the Present Finding

The present experiment has shown that the normal cellular PrP^{C} and the infectious form, PrP^{Sc} are interconvertible by pressure. Namely, an equilibrium holds basically between PrP^{Sc} and PrP^{C}, namely $PrP^{Sc} \rightleftharpoons PrP^{C}$. Accordingly, we may conclude that the crucial molecular event of the prion disease is also likely to be a thermodynamically controlled process.

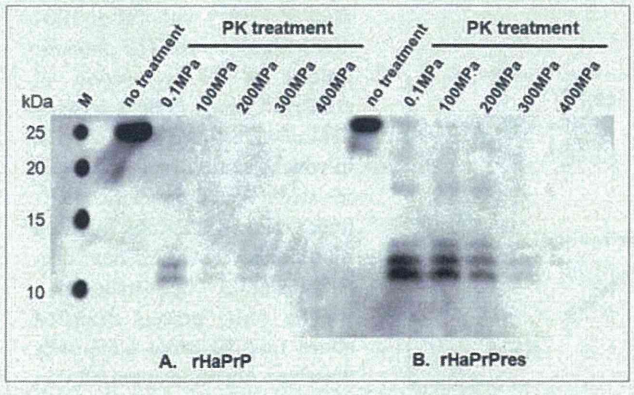

Figure 3. Western blotting of rHaPrP and rHaPrP^{res} fibrils PK-treated under different pressures. (**A**) rHaPrP treated with proteinase K at different pressures at 25 °C for 1 h. (**B**) rHaPrP^{res} fibrils treated with proteinase K at different pressures at 25 °C for 1 h See Materials and Methods for more details.

This conclusion does not depend, in essence, on whether some complex reactions and/or intermediates are involved or not in this overall equilibrium above. The conclusion is particularly important, as it means that the reversible nature of the fibril-forming reaction, found in much simpler amyloidogenic protein systems so far studied,[9-13] is now extended to the highly heterogeneous assembly of fibrils of rHaPrP^{res} such as those seen in **Figure 2A**. Furthermore, the present result, showing the increase in the monomer fraction with increasing pressure, implies that, under closely physiological conditions, the partial molar volume of the prion protein is smaller in the monomeric state, PrP^{C}, than in the fibrous state, PrP^{Sc}, namely $\Delta V = V_{monomer} - V_{fibril} < 0$. This places pressure as a useful general tool for controlling the PrP^{C}-PrP^{Sc} conversion, prompting us to carry on further detailed analysis of the conversion reaction between PrP^{C} and PrP^{Sc} based on the thermodynamic and/or kinetic approach.

Technically, the method of pressure-accelerated proteolysis combined with western blotting introduced here is a novel approach generally applicable to the thermodynamic and kinetic analyses of various bio-macromolecular systems of high degree of association, for many of which a normal spectroscopic approach would fail because of the low sensitivity of detection and because of the slowness of the reaction at ambient conditions. In practice, the dramatic pressure effect on increasing the PK-digestibility of otherwise "PK-resistant" prion fibrils within a moderate range of pressure (< a few hundred MPa) suggests a simple and efficient means of eliminating infectious PrP^{Sc} from various systems in vitro.

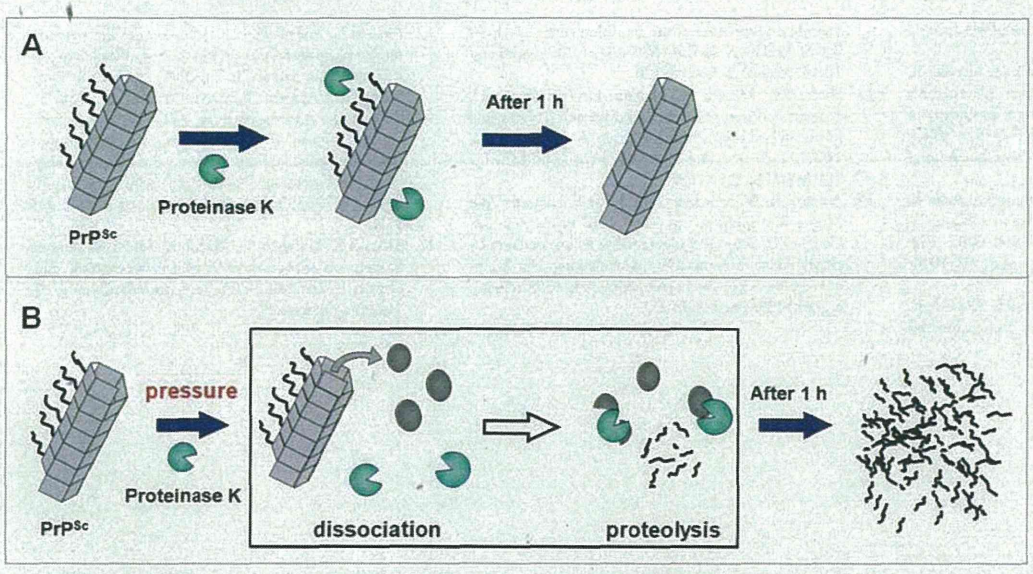

Figure 4. Illustration of the molecular events in the PK-treatment of rHaPrP^{res} fibrils. (**A**) At 0.1 MPa, where no dissociation of fibrous rHaPrP^{res} takes place, only the flexible N-terminal segments (residues 23 to 140) are cleaved off by proteinase K, leaving the fibril consisting only of the core parts (residues ~141 to 231). (**B**) At high pressures (100–400 MPa), fibrous rHaPrP^{res} dissociates into monomeric rHaPrP one by one, which is then readily degraded by proteinase K.

Materials and Methods

Preparation of rHaPrP^{res} fibrils

Fibrils of rHaPrP^{res} were prepared from recombinant hamster prion protein (rHaPrP [23–231]) by shaking with brain homogenate of scrapie-infected hamster at 25 °C in 0.5 M Gdn-HCl, 150 mM NaCl, 150 mM HEPES buffer, pH 7.0 (QUIC).[14]

Proteolysis of rHaPrP^{res}

For the proteolysis reaction, the above solution containing rHamPrP^{res} was diluted with pure water by 2.5-fold, making the final solution containing 40μg/ml of rHamPrP^{C}, to which proteinase K was added to the concentration of 10μg /ml in 0.2 M Gdn-HCl, 60 mM NaCl, 60 mM HEPES, pH 7.0. Each 30μl of the above mixture, held in a tiny Teflon tube placed within a home-made pressure vessel, was subjected to a pressure ranging from 0.1 MPa to 400 MPa at 25 °C for 1 h. After the reaction was completed, 22μl of each solution was used for western blotting and the rest for atomic force microscopy (AFM) measurement.

Western blotting

The resultant solutions were subjected to western blotting with an anti PrP-goat polyclonal IgG, specific to residues 121–231 as primary antibody and alkaline phosphatase (AP) -anti-Goat IgG as secondary antibody. M refers to the lane for the molecular weight marker.

Atomic force microscopy

For each PK-treated samples, 2 μl of the solution was applied on a new mica surface, rinsed with pure water, and dried. AFM figures of fibrils were recorded with a cyclic contact mode at a frequency of 128 kHz on SPI-3800 scanning probe microscopy (Seiko Instruments Inc.).

Disclosure of Potential Conflicts of Interest

No potential conflicts of interest were disclosed.

Acknowledgments

This work was performed under the auspicies of the Academic Frontier Program 07F010 (Kinki University) and the Global COE Program (Nagasaki University) from the Ministry of Education, Culture, Sports, Science and Technology of Japan (MEXT) and supported in part by a Grant-in-Aid for Scientific Research (C) No.24570180. We thank I. Ichimiya of Science Technology Interact Co., LTD for her help in organizing the collaboration in this work.

References

1. Prusiner SB. Prions. Proc Natl Acad Sci U S A 1998; 95:13363-83; PMID:9811807; http://dx.doi.org/10.1073/pnas.95.23.13363
2. Bocharova OV, Makarava N, Breydo L, Anderson M, Salnikov VV, Baskakov IV. Annealing PrP fibrils at high temperature results in extension of a proteinase K resistant core. J Biol Chem 2006; 281:2373-9; PMID:16314415; http://dx.doi.org/10.1074/jbc.M510840200
3. Race R, Jenny A, Sutton D. Scrapie infectivity and proteinase K-resistant prion protein in sheep placenta, brain, spleen, and lymph node: implications for transmission and antemortem diagnosis. J Infect Dis 1998; 178:949-53; PMID:9806020; http://dx.doi.org/10.1086/515669
4. Akasaka K. Probing conformational fluctuation of proteins by pressure perturbation. Chem Rev 2006; 106:1814-35; PMID:16683756; http://dx.doi.org/10.1021/cr040440z
5. Silva JL, Weber G. Pressure stability of proteins. Annu Rev Phys Chem 1993; 44:89-113; PMID:8257561; http://dx.doi.org/10.1146/annurev.pc.44.100193.000513
6. Royer CA. Revisiting volume changes in pressure-induced protein unfolding. Biochim Biophys Acta 2002; 1595:201-9; PMID:11983396; http://dx.doi.org/10.1016/S0167-4838(01)00344-2
7. Cordeiro Y, Kraineva J, Winter R, Silva JL. Volume and energy folding landscape of prion protein revealed by pressure. Braz J Med Biol Res 2005; 38:1195-201; PMID:16082459; http://dx.doi.org/10.1590/S0100-879X2005000800006
8. Sasaki K, Gaikwad J, Hashiguchi S, Kubota T, Sugimura K, Kremer W, Kalbitzer HR, Akasaka K. Reversible monomer-oligomer transition in human prion protein. Prion 2008; 2:118-22; PMID:19158507; http://dx.doi.org/10.4161/pri.2.3.7148
9. Akasaka K, Latif AR, Nakamura A, Matsuo K, Tachibana H, Gekko K. Amyloid protofibril is highly voluminous and compressible. Biochemistry 2007;

46:10444-50; PMID:17715944; http://dx.doi.org/10.1021/bi700648b
10. Niraula TN, Konno T, Li H, Yamada H, Akasaka K, Tachibana H. Pressure-dissociable reversible assembly of intrinsically denatured lysozyme is a precursor for amyloid fibrils. Proc Natl Acad Sci U S A 2004; 101:4089-93; PMID:15016916; http://dx.doi.org/10.1073/pnas.0305798101
11. Kamatari YO, Yokoyama S, Tachibana H, Akasaka K. Pressure-jump NMR study of dissociation and association of amyloid protofibrils. J Mol Biol 2005; 349:916-21; PMID:15907935; http://dx.doi.org/10.1016/j.jmb.2005.04.010
12. Abdul Latif AR, Kono R, Tachibana H, Akasaka K. Kinetic analysis of amyloid protofibril dissociation and volumetric properties of the transition state. Biophys J 2007; 92:323-9; PMID:16997869; http://dx.doi.org/10.1529/biophysj.106.088120
13. Shah BR, Maeno A, Matsuo H, Tachibana H, Akasaka K. Pressure-accelerated dissociation of amyloid fibrils in wild-type hen lysozyme. Biophys J 2012; 102:121-6; PMID:22225805; http://dx.doi.org/10.1016/j.bpj.2011.10.041
14. Atarashi R, Wilham JM, Christensen L, Hughson AG, Moore RA, Johnson LM, Onwubiko HA, Priola SA, Caughey B. Simplified ultrasensitive prion detection by recombinant PrP conversion with shaking. Nat Methods 2008; 5:211-2; PMID:18309304; http://dx.doi.org/10.1038/nmeth0308-211
15. Akasaka K, Yamada H. (2001) On-line cell high pressure nuclear magnetic resonance technique: Application to protein studies. In: James TL, Ed.(2001) Methods in Enzymology 338, Academic Press, New York, pp 134-158.
16. Torrent J, Alvarez-Martinez MT, Harricane MC, Heitz F, Liautard JP, Balny C, Lange R. High pressure induces scrapie-like prion protein misfolding and amyloid fibril formation. Biochemistry 2004; 43:7162-70; PMID:15170353; http://dx.doi.org/10.1021/bi049939d
17. Akasaka K, Nagahata H, Maeno A, Sasaki K. Pressure acceleration of proteolysis. A general mechanism. Biophysics (Oxf) 2008; 4:29-32; http://dx.doi.org/10.2142/biophysics.4.29

Journal of Virology

Conformational Properties of Prion Strains Can Be Transmitted to Recombinant Prion Protein Fibrils in Real-Time Quaking-Induced Conversion

Kazunori Sano, Ryuichiro Atarashi, Daisuke Ishibashi, Takehiro Nakagaki, Katsuya Satoh and Noriyuki Nishida
***J. Virol.* 2014, 88(20):11791. DOI: 10.1128/JVI.00585-14.**
Published Ahead of Print 30 July 2014.

JVI
Journals.ASM.org

Conformational Properties of Prion Strains Can Be Transmitted to Recombinant Prion Protein Fibrils in Real-Time Quaking-Induced Conversion

Kazunori Sano,[a] Ryuichiro Atarashi,[a,b] Daisuke Ishibashi,[a] Takehiro Nakagaki,[a] Katsuya Satoh,[a] Noriyuki Nishida[a]

Department of Molecular Microbiology and Immunology, Nagasaki University Graduate School of Biomedical Sciences, Nagasaki, Japan[a]; Research Centre for Genomic Instability and Carcinogenesis, Nagasaki University, Nagasaki, Japan[b]

ABSTRACT

The phenomenon of prion strains with distinct biological characteristics has been hypothesized to be involved in the structural diversity of abnormal prion protein (PrP^{Sc}). However, the molecular basis of the transmission of strain properties remains poorly understood. Real-time quaking-induced conversion (RT-QUIC) is a cell-free system that uses *Escherichia coli*-derived recombinant PrP (rPrP) for the sensitive detection of PrP^{Sc}. To investigate whether the properties of various prion strains can be transmitted to amyloid fibrils consisting of rPrP (rPrP fibrils) using RT-QUIC, we examined the secondary structure, conformational stability, and infectivity of rPrP fibrils seeded with PrP^{Sc} derived from either the Chandler or the 22L strain. In the first round of the reaction, there were differences in the secondary structures, especially in bands attributed to β-sheets, as determined by infrared spectroscopy, and conformational stability between Chandler-seeded (1st-rPrP-fib^{Ch}) and 22L-seeded (1st-rPrP-fib^{22L}) rPrP fibrils. Of note, specific identifying characteristics of the two rPrP fibril types seen in the β-sheets resembled those of the original PrP^{Sc}. Furthermore, the conformational stability of 1st-rPrP-fib^{Ch} was significantly higher than that of 1st-rPrP-fib^{22L}, as with Chandler and 22L PrP^{Sc}. The survival periods of mice inoculated with 1st-rPrP-fib^{Ch} or 1st-rPrP-fib^{22L} were significantly shorter than those of mice inoculated with mixtures from the mock 1st-round RT-QUIC procedure. In contrast, these biochemical characteristics were no longer evident in subsequent rounds, suggesting that nonspecific uninfected rPrP fibrils became predominant probably because of their high growth rate. Together, these findings show that at least some strain-specific conformational properties can be transmitted to rPrP fibrils and unknown cofactors or environmental conditions may be required for further conservation.

IMPORTANCE

The phenomenon of prion strains with distinct biological characteristics is assumed to result from the conformational variations in the abnormal prion protein (PrP^{Sc}). However, important questions remain about the mechanistic relationship between the conformational differences and the strain diversity, including how strain-specific conformations are transmitted. In this study, we investigated whether the properties of diverse prion strains can be transmitted to amyloid fibrils consisting of *E. coli*-derived recombinant PrP (rPrP) generated by real-time quaking-induced conversion (RT-QUIC), a recently developed *in vitro* PrP^{Sc} formation method. We demonstrate that at least some of the strain-specific conformational properties can be transmitted to rPrP fibrils in the first round of RT-QUIC by examining the secondary structure, conformational stability, and infectivity of rPrP fibrils seeded with PrP^{Sc} derived from either the Chandler or the 22L prion strain. We believe that these findings will advance our understanding of the conformational basis underlying prion strain diversity.

Prion diseases, or transmissible spongiform encephalopathies (TSEs), are infectious and fatal neurodegenerative disorders characterized by progressive spongiform changes and the accumulation of abnormal prion protein (PrP^{Sc}) in the central nervous system. Although the pathogenic mechanisms have not been fully elucidated, prion disease is thought to occur through autocatalytic conversion of normal prion protein (PrP^{C}) to PrP^{Sc} (1, 2), known as the protein-only hypothesis. Some biophysical properties are known to differ between PrP^{C} and PrP^{Sc}. PrP^{C} is monomeric, detergent soluble, and protease sensitive, while PrP^{Sc} is polymeric, detergent insoluble, and partially protease resistant (3). These differences are most likely due to the different conformations of the two isoforms. PrP^{C} is largely α-helical, whereas PrP^{Sc} is substantially enriched in β-sheets (4, 5), frequently resulting in amyloid fibril formation.

The existence of diverse prion strains in mammalian species manifesting as phenotypic differences is well-known. The strain-specific characteristics are usually maintained upon serial passage in the same species and may be explained by conformational variations in PrP^{Sc}. Indeed, strain-dependent differences in β-sheet-rich structures of PrP^{Sc} have been demonstrated by infrared spectroscopy (6–9). In addition, the conformational stability of PrP^{Sc} differs among prion strains, as demonstrated by a guanidine hydrochloride (GdnHCl) denaturation assay followed by protease digestion (10, 11). However, the mechanistic relationship between

Received 26 February 2014 Accepted 26 July 2014
Published ahead of print 30 July 2014
Editor: B. W. Caughey
Address correspondence to Ryuichiro Atarashi, atarashi@nagasaki-u.ac.jp.

doi:10.1128/JVI.00585-14

PrP^{Sc} conformational differences and the molecular basis of prion strains remains poorly understood.

Various *in vitro* PrP^{Sc} formation methods have been developed to elucidate the pathogenesis of prion diseases. One of these methods, protein misfolding cyclic amplification (PMCA), enabled the exponential amplification of PrP^{Sc} *in vitro* by sonication-induced fragmentation of large PrP^{Sc} polymers into smaller units (12). An increase in the infectivity of PrP^{Sc} amplified by PMCA was obtained by using brain homogenate (BH) from healthy mice (normal brain homogenate [NBH]) as a source of PrP^{C} substrates (BH-PMCA) (13). Furthermore, PrP^{Sc} generated by BH-PMCA from five different mouse prion strains retained the strain-specific properties (14). In addition, prion infectivity could be propagated when purified brain-derived PrP^{C} or baculovirus-derived PrP^{C} was used as the substrate in the presence of certain cofactors, such as nucleic acids and BH from PrP-deficient mice (15–17). These results provide strong evidence to support the protein-only hypothesis, but the structural basis of prion pathogenesis, including the tertiary structure of PrP^{Sc}, has not been fully clarified.

On the other hand, the use of *Escherichia coli*-derived purified recombinant PrP (rPrP) offers an advantage over the use of conformational analyses, which generally require target protein of high purity and a large quantity of the target protein. Spontaneously polymerized amyloid fibrils of rPrP have been reported to induce the accumulation of PrP^{Sc} in the brains of PrP-overexpressing transgenic (Tg) mice (18–20) and some wild-type hamsters (21); however, the incubation periods spanned no less than several hundred days, and none of the wild-type hamsters developed any neurological signs at first passage, indicating that the level of infectivity generated in these studies is very low. More recently, wild-type mice developed clinical disease typical of TSE at about 130 days after injection of proteinase K (PK)-resistant rPrP fibrils generated by unseeded PMCA in the presence of 1-palmitoyl-2-oleoylphosphatidylglycerol (POPG), a synthetic lipid molecule, and total liver RNA (22). Although these results were reproduced by the same group (23), others have reported that rPrP fibrils generated by the same method were unable to induce either neuropathological changes or the accumulation of PrP^{Sc} (24). Thus, the role of POPG and RNA in the *de novo* generation of infectious rPrP fibrils remains controversial.

Meanwhile, two different seeded PMCA reaction studies using rPrP as a substrate (rPrP-PMCA) have demonstrated the propagation of moderate levels of prion infectivity. One study showed that hamster rPrP can be converted to rPrP fibrils capable of inducing TSE in the presence of SDS, a synthetic anionic detergent, but there were great variations in the attack rate and the incubation period, which ranged from 119 to 401 days (25). Another study revealed that phosphatidylethanolamine (PE), a phospholipid found in biological membranes, enhances the conversion of mouse rPrP into rPrP fibrils capable of inducing TSE after about 400 days of incubation with a 100% attack rate (26, 27). Of note, three different strains used as a seed were converted into a single strain with unique properties during the serial rPrP-PMCA experiments (27). These studies suggest that a certain amphipathic molecule, such as PE, is a cofactor required for the propagation of prion infectivity *in vitro* but not for the transmission of strain-specific properties.

The recently developed real-time (RT) quaking-induced conversion (QUIC) is a sensitive prion detection method (28, 29) in which intermittent shaking enhances the conversion of soluble rPrP into amyloid fibrils in the presence of PrP^{Sc}. The aim of the present research was to investigate whether properties of diverse prion strains can be transmitted to rPrP fibrils generated in the RT-QUIC system. We produced proteinase K-resistant rPrP fibrils seeded with minute quantities of mouse-adapted scrapie (Chandler or 22L strain) PrP^{Sc} and investigated the secondary structure, conformational stability, and infectivity.

MATERIALS AND METHODS

Mouse rPrP expression and purification. Recombinant PrP (rPrP) equivalent to residues 23 to 231 of the mouse PrP sequence was expressed, refolded into a soluble form, and purified essentially as previously described (30). The concentration of rPrP was determined by measuring the absorbance at 280 nm. The purity of the final protein preparations was ≥99%, as estimated by SDS-PAGE, immunoblotting, and liquid chromatography-mass spectrometry (data not shown). After purification, aliquots of the proteins were stored at −80°C in 10 mM phosphate buffer, pH 6.8, or distilled water.

Preparation of brain homogenates. Brain tissues were homogenized at 10% (wt/vol) in ice-cold phosphate-buffered saline (PBS) supplemented with a protease inhibitor mixture (Roche) using a multibead shocker (Yasui Kikai, Osaka, Japan). After centrifugation at 2,000 × *g* for 2 min, supernatants were collected and frozen at −80°C until use. Total protein concentrations were determined by the bicinchoninic acid protein assay (Pierce). The PrP^{Sc} concentrations in the brain homogenates were estimated by dot blot analysis using a reference standard of rPrP, as previously described (31).

RT-QUIC experiments. We prepared reaction mixtures in a 96-well, optical, black-bottom plate (catalog number 265301; Nunc) to a final total volume of 100 μl. To avoid contamination, we prepared noninfectious materials inside a biological safety cabinet in a prion-free laboratory and used aerosol-resistant tips. The final concentrations of the reaction buffer components were 300 mM NaCl, 50 mM HEPES, pH 7.5, and 10 μM thioflavin T (ThT). The concentration of rPrP was 50 or 100 μg/ml, and only freshly thawed rPrP was used. Brain homogenate was diluted with reaction buffer prior to the reactions. The 96-well plate was covered with sealing tape (catalog number 236366; Nunc) and incubated at 40°C in a plate reader (Infinite M200 fluorescence plate reader; Tecan) with intermittent shaking consisting of 30 s of circular shaking at the highest speed and no shaking for 30 s and then with a 2-min pause to measure the fluorescence. The kinetics of amyloid formation was monitored by reading of the fluorescence intensity on the bottom of the plate every 10 min using monochromators with 440-nm excitation and 485-nm emission wavelengths.

RT-QUIC product analysis. For detection of protease-resistant rPrP, 10 μl of the QUIC samples (1 μg of rPrP) was diluted with 40 μl of buffer (300 mM NaCl, 50 mM HEPES, pH 7.5) and digested with 10 μg/ml of PK at 37°C for 1 h. After adding 4-(2-aminoethyl)benzenesulfonyl fluoride hydrochloride (Pefabloc; Roche) at a final concentration of 4 mM and 20 μg of thyroglobulin, the proteins were precipitated with 4 volumes of methanol. The samples were heated in sample buffer (2% SDS, 5% β-mercaptoethanol, 5% sucrose, 0.005% bromophenol blue, 62.5 mM Tris-HCl, pH 6.8) at 95°C for 5 min and then loaded onto 10% bis-Tris NuPAGE gels (Invitrogen). Proteins were transferred onto polyvinylidene difluoride membranes (Millipore, Billerica, MA). The membranes were probed with polyclonal anti-PrP antibody R20 (the epitope located at mouse PrP amino acids 218 to 231) or ICSM35 (D-Gen, London, United Kingdom).

TEM. Negative staining was done on carbon supporting film grids, which were glow discharged before staining. The 10-μl samples were adsorbed to the grids for 3 min, and then the residual solution was absorbed by filter paper. The grids were stained with 20 μl of fleshly filtered stain (2% uranyl acetate). Once they were dry, the samples were viewed in a transmission electron microscope (TEM; JEM-1200EX; JEOL, Japan).

FTIR. Fourier transform infrared spectroscopy (FTIR) spectra were measured with a Bruker Tensor 27 FTIR instrument (Bruker Optics) equipped with a mercuric cadmium telluride (MCT) detector cooled with liquid nitrogen. Three hundred microliters of each of the QUIC samples (30 μg of rPrP) was pelleted by centrifugation for 1 h at 77,000 × *g* and resuspended in 20 μl buffer (300 mM NaCl, 50 mM HEPES, pH 7.5). The slurry was loaded into a BioATRcell II attenuated total reflectance-type reflectance unit. PrP^{Sc} was purified from the brains of mice infected with the mouse-adapted Chandler and 22L prions using a combination of detergent solubilization, centrifugation at ultrahigh speeds, and PK digestion (4, 32), and 15 μl of purified PrP^{Sc} was directly loaded. One hundred twenty-eight scans at a 4-cm^{-1} resolution were collected for each sample under constant purging with nitrogen, corrected for water vapor, and the background spectra of the buffer were subtracted.

Conformational stability assay. Ten microliters of the QUIC products (equivalent to 1 μg of rPrP) and brain homogenates (80 μg of total proteins) was mixed with 22 μl of various concentrations of guanidine hydrochloride (GdnHCl) at final concentrations of 0 to 5 M and 0 to 3.5 M, respectively, and the mixed samples were incubated at 37°C for 1 h. After adjustment of the final GdnHCl concentration of the QUIC products to 1 M and the brain homogenates to 0.6 M, the samples were digested with PK (10 μg/ml) at 37°C for 1 h and analyzed by Western blotting following methanol precipitation. The bands were visualized using an Attophos AP fluorescent substrate system (Promega) and quantified using a Molecular Imager FX imager (Bio-Rad). The sigmoidal patterns of the denaturation curves were plotted using a Boltzmann curve fit. The concentration of GdnHCl required to denature 50% of PK-resistant fragments ($[GdnHCl]_{1/2}$) was estimated from the denaturation curves.

Bioassay. Four-week-old male ddY mice were intracerebrally inoculated with 40 μl of QUIC products (equivalent to 4 μg rPrP). As controls for rPrP fibrils, we performed a mock QUIC procedure using seed-only solutions that contained the same concentration of PrP^{Sc} as that from the 1st round of QUIC with the rPrP fibril (1st-rPrP-fibril; 1 pg/μl) or the 5th round of QUIC with the rPrP fibril (5th-rPrP-fibril; 1×10^{-8} pg/μl) and then added the same amount of rPrP and inoculated the mixtures into mice. Brain homogenates were serially diluted from 10^0 to 10^{-7} with PBS, and 20 μl of each dilution was intracerebrally inoculated. Mice were monitored weekly until the terminal stage of disease or sacrifice. Clinical onset was determined as the presence of 3 or more of the following signs: greasy and/or yellowish hair, hunchback, weight loss, yellow pubes, ataxic gait, and nonparallel hind limbs. The 50% lethal dose (LD_{50}) was determined according to the Behrens-Karber formula. Animals were cared for in accordance with the guidelines for animal experimentation of Nagasaki University.

Histopathology and lesion profiles. The brain tissue was fixed in 4% paraformaldehyde, and 5-μm paraffin sections were prepared on poly-L-lysine (PLL) coat slides using a microtome. After deparaffinization and rehydration, the tissue sections were stained with hematoxylin-eosin. The pattern of vacuolation was examined in 8 fields per slice from the hippocampus (HI), cerebral cortex, hypothalamus, pons, and cerebellum (CE). Spongiform degeneration was scored using the following scale: 0, no vacuoles; 1, a few vacuoles widely and unevenly distributed; 2, a few vacuoles evenly scattered; 3, moderate numbers of vacuoles evenly scattered; 4, many vacuoles with some confluences; and 5, dense vacuolation.

Statistical analysis. The fibril length or width determined by electron microscopy analysis was subjected to one-way analysis of variance (ANOVA) followed by the Tukey-Kramer test. Data from the conformational stability test were analyzed by one-way ANOVA followed by Student's *t* test. Analysis of the data for the survival times was evaluated by the log-rank test. The vacuolation scores were analyzed by Mann-Whitney's U test.

RESULTS

Conversion of the soluble form of mouse rPrP into amyloid fibrils by RT-QUIC. We first tested whether formation of mouse rPrP amyloid fibrils could be induced in the RT-QUIC by monitoring the levels of ThT fluorescence. We observed positive ThT fluorescence in the presence of diluted strain Chandler-seeded brain homogenate (BH) or strain 22L-seeded BH containing 100 pg of PrP^{Sc} (Fig. 1A), whereas negative-control reactions seeded with comparable dilutions of BH from healthy mice (normal brain homogenate [NBH]) or not seeded resulted in no increase in ThT fluorescence over 72 h (Fig. 1A). However, because an inverse correlation existed between the rate of fibril formation and the concentration of rPrP (28, 33), the spontaneous formation of rPrP fibrils (rPrP-fib^{spon}) was induced by decreasing the concentration of rPrP from 100 to 50 μg/ml (Fig. 1A).

We next examined the PK resistance of rPrP fibrils by immunoblotting using anti-PrP antibody R20 directed toward C-terminal residues 218 to 231. Although the ThT-negative reactions seeded with NBH or not seeded produced no PK-resistant bands (Fig. 1B, middle), the Chandler-seeded rPrP fibrils (rPrP-fib^{Ch}) and 22L-seeded rPrP fibrils (rPrP-fib^{22L}) produced several (21-, 18-, 12-, 11-, and 10-kDa) PK-resistant fragments (Fig. 1B, left). In contrast, the PK digestion of rPrP-fib^{spon} generated only 10- to 12-kDa fragments. It should be noted that anti-PrP monoclonal antibody ICSM35 (directed toward an epitope consisting of residues 93 to 102) specifically recognized the 21- and 18-kDa fragments derived from PrP^{Sc}-seeded rPrP fibrils in the first round (1st-rPrP-fib^{Sc}), indicating that they contained mouse PrP from about residues 93 to 231 (Fig. 1B, right).

To further characterize the structure of 1st-rPrP-fib^{Sc} and rPrP-fib^{spon}, the samples were examined using a TEM with negative staining. The electron micrographs of samples of 1st-rPrP-fib^{Ch} and 1st-rPrP-fib^{22L} revealed bundles of irregularly rod-shaped and branched fibrils, while most samples of rPrP-fib^{spon} displayed smooth and nonbranched rod-shaped fibrils (Fig. 1C). Moreover, the lengths of 1st-rPrP-fib^{Ch} and 1st-rPrP-fib^{22L} were significantly longer than those of rPrP-fib^{spon} (Fig. 1D). Thus, the results of TEM analysis suggest that 1st-rPrP-fib^{Sc} are structurally distinct from spontaneous rPrP-fib^{spon}.

We next examined the morphology of PrP^{Sc}-seeded rPrP fibrils in the 2nd- and 5th-round reactions (2nd- and 5th-rPrP-fib^{Sc}, respectively) by TEM. In contrast to samples of 1st-rPrP-fib^{Sc}, samples of 2nd- and 5th-rPrP-fib^{Sc} displayed spindly and nonbranched fibrils or amorphous aggregates (Fig. 2). These data support the view that 1st-rPrP-fib^{Sc} are structurally distinct from 2nd- and 5th-rPrP fib^{Sc}.

Structural characterization of rPrP fibrils by FTIR. We next examined the secondary structure of rPrP fibrils and purified PrP^{Sc} from the brains of mice infected with Chandler or 22L scrapie by FTIR. A silver-stained SDS-polyacrylamide gel analysis revealed that Chandler and 22L PrP^{Sc} preparations were highly purified (Fig. 3A). Furthermore, TEM analysis demonstrated that the PrP^{Sc} preparations consisted exclusively of amyloid-like fibrils (Fig. 3B). FTIR analysis showed that Chandler PrP^{Sc} was characterized by a major band at 1,630 cm^{-1} in the β-sheet region of second-derivative spectra, while 22L PrP^{Sc} was characterized by two absorbance bands at 1,631 and 1,616 cm^{-1} (Fig. 4A), indicating that there were conformational differences in the β-sheet structures between Chandler and 22L PrP^{Sc}, as previously reported (7). Consistent with previous reports (6–9), bands of about 1,656 to 1,658 cm^{-1} were observed in both Chandler and 22L PrP^{Sc}. Although these bands were formerly attributed to an α-helix, recent studies using direct mass spectrometric analysis of hy-

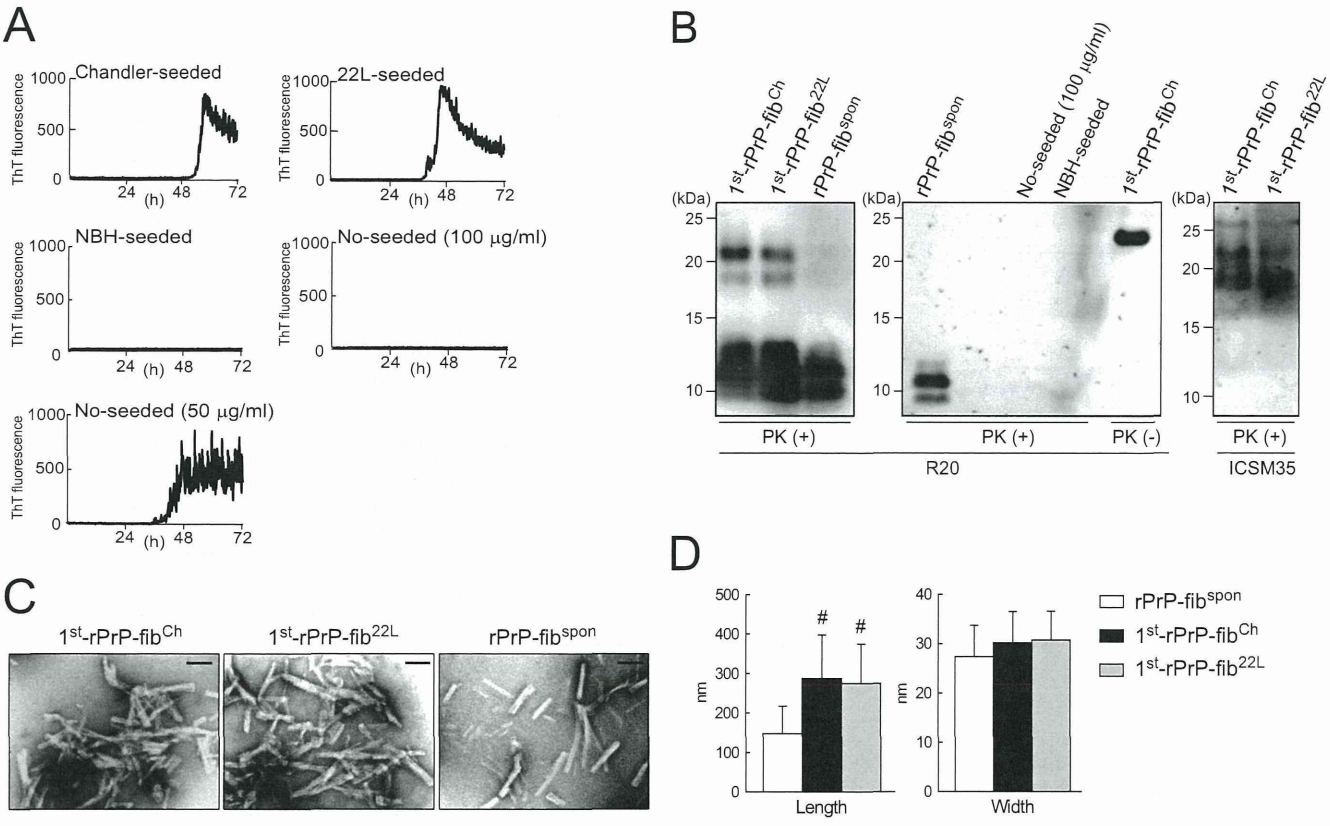

FIG 1 Formation of rPrP fibrils in RT-QUIC reactions. (A) The formation of rPrP fibrils in the presence of diluted Chandler or 22L BH containing 100 pg of PrP^{Sc} or a comparable amount of NBH or in the absence of seed (No-seeded) was monitored by measurement of ThT fluorescence. The graphs depict representative results of the RT-QUIC reactions. No-seed reactions were performed at two different concentrations (100 or 50 μg/ml) of rPrP. (B) The QUIC reaction mixtures were digested with PK and immunoblotted using polyclonal anti-PrP antibody R20 (specific for the epitope located at mouse PrP amino acids 218 to 231) or ICSM35 (specific for the epitope located at mouse PrP amino acids 93 to 102). For comparison, 1st-rPrP-fib^{Ch} (50 ng of total rPrP) without PK digestion [PK (−)] is shown. Molecular mass markers are indicated in kilodaltons (kDa) on the left side of each panel. (C) Samples (1st-rPrP-fib^{Ch}, 1st-rPrP-fib^{22L}, and rPrP-fib^{spon}) were examined by TEM. Bars, 100 nm. (D) The bar graph shows the length and width of rPrP-fib^{spon}, 1st-rPrP-fib^{Ch}, and 1st-rPrP-fib^{22L}. The results are the mean ± SD for 30 rPrP fibrils each. Statistical significance was determined using one-way ANOVA, followed by the Tukey-Kramer test. *, $P < 0.01$.

drogen-deuterium exchange and FTIR analysis have suggested that purified PrP^{Sc} has little α-helix content and the bands probably result from turns (9, 34). Native rPrP had a maximum absorbance at 1,653 cm^{-1}, which was congruent with that of prominent α-helical structures. In contrast, all rPrP fibrils displayed prominent bands at lower wave numbers (1,630 to 1,610 cm^{-1}), indicating a predominantly β-sheet content (Fig. 4A). The β-sheet spectra revealed conformational differences among rPrP-fib^{spon}, 1st-rPrP-fib^{Ch}, and 1st-rPrP-fib^{22L}. rPrP-fib^{spon} had a prominent band at 1,623 cm^{-1} and a modest band at 1,610 cm^{-1}. While the 1st-rPrP-fib^{Ch} were characterized by a single major band at 1,624 cm^{-1}, the 1st-rPrP-fib^{22L} had two major maxima at 1,629 and 1,617 cm^{-1} (Fig. 4A). Although 1st-rPrP-fib^{Sc} lacked the bands at about 1,656 to 1,658 cm^{-1}, the strain-specific shapes (one peak in Chandler versus two peaks in 22L) in the β-sheet spectrum of the purified PrP^{Sc} resembled those of 1st-rPrP-fib^{Sc}.

To test whether the strain-specific infrared spectra observed in 1st-rPrP-fib^{Ch} and 1st-rPrP-fib^{22L} are transmitted to sequential QUIC reactions, we performed 5 serial rounds of QUIC (Fig. 2A). There was little difference in the β-sheet spectra between 5th-rPrP-fib^{Ch} and 5th-rPrP-fib^{22L} (Fig. 3), suggesting that strain-specific conformations were lost in the 5th-rPrP-fib^{Sc}. Furthermore, additional experiments revealed that the infrared spectra of rPrP fibrils produced in the presence of a small amount of PrP^{Sc} (1 pg) or under acidic conditions (pH 4) displayed few differences between strains (Fig. 4B).

Conformational stability analysis of rPrP fibrils and PrP^{Sc}. To examine the biochemical differences of rPrP fibrils and PrP^{Sc} in BH between strains, we performed a conformational stability assay, which combines GdnHCl denaturation with PK digestion. The $[GdnHCl]_{1/2}$ values for Chandler and 22L PrP^{Sc} were 3.3 ± 0.4 and 1.7 ± 0.3 M, respectively (Fig. 5A and Table 1), indicating that the conformational stability of Chandler-PrP^{Sc} was significantly higher than that of 22L-PrP^{Sc}. Consistent with previous work (11), Chandler PrP^{Sc} bands treated with more than 1.5 M GdnHCl were approximately 5 kDa smaller than those treated with lower concentrations (Fig. 5A, top). The $[GdnHCl]_{1/2}$ values of 1st-rPrP-fib^{Ch} and 1st-rPrP-fib^{22L} were 3.3 ± 0.1 and 2.3 ± 0.6 M, respectively (Fig. 5B and Table 1), showing that the stability of 1st-rPrP-fib^{Ch} was significantly higher than that of 1st-rPrP-fib^{22L}, as with Chandler and 22L PrP^{Sc}. Thus, the relationship between Chandler and 22L in terms of conformational stability was common to both the original PrP^{Sc} and 1st-rPrP-fib^{Sc}. In contrast, the $[GdnHCl]_{1/2}$ of rPrP-fib^{spon} was more than 5 M,